Modeling hypertrophic cardiomyopathy mutations in neonatal cardiomyocytes cultured in 3D

Esther S. Choi

Molecular, Cellular, and Developmental Biology

Departmental Honors Thesis

University of Colorado, Boulder

Thesis Advisors:

Dr. Leslie Leinwand (MCDB)

Dr. Kristi Anseth (Chemical and Biological Engineering)

Honors Council Representative:

Dr. Pamela Harvey (MCDB)

Abstract

Heart disease continues to be the leading cause of death in both men and women. It is accompanied with cellular- and organ- level remodeling that cannot be mimicked or recaptured by cells on standard culture platforms. Polyethylene glycol hydrogels bridge this gap by providing user-defined tunability for cell culture. A novel 3D cell culture system was developed to encapsulate neonatal rat ventricular cardiomyocytes (NRVMs) in a single plane, and cell health was assessed. In parallel, recombinant adenoviruses containing the mutations responsible for human hypertrophic cardiomyopathy (HCM) in the beta myosin gene (R403Q and R453C) were generated and used as a tool to study the acute effects of HCM. Expression and incorporation of the HCM mutant myosins in NRVMs were sufficient to cause a cellular disease phenotype; this work presents initial characterizations of the morphological, functional, and molecular differences. Cells cultured in 3D were viable and presented a heathly baseline for cardiomyocytes. This merits further studies to implement a 3D cell culture system to more accurately assess cellular disease characteristics. Disease progression can be deconvoluted if the characteristics are compared to a baseline that more appropriately resembles the healthy native tissue. This work and the possible future studies provide a foundation for better disease characterizations that can promote effective drug development.

1. Introduction

Hypertrophic cardiomyopathy (HCM) is best known among the public as the primary cause of sudden cardiac death in young athletes. It is the most frequent genetic cause of heart disease, present in roughly 1 in 500 adults. HCM is typically a monogenic, dominantly inherited disease and many different causative mutations have been identified. Most causative mutations are in genes that encode for the proteins that make up the sarcomere (Richard, 2003).The sarcomere is the functional contractile unit of a muscle and over 1,000 sarcomere protein mutations have been implicated in HCM (Seidman & Seidman, 2011). The primary diagnostic criterium is unexplained left ventricular hypertrophy (LVH) due to cellular growth of the cardiac myocyte (Harvey & Leinwand, 2011). There is high variability in the phenotypic penetrance of HCM that can make spontaneous cases difficult to identify prior to the appearance of severe impairments. Moreover, it is most commonly diagnosed in adulthood or post-mortem, in part due to the difficulty in identifying the early stages of the disease. In some cases, HCM may be identified in infants and young children. These very severe cases are thought to be caused by the same mutations that cause the appearance of the disease in adults (Kaski et al., 2009; Morita et al., 2008).

In addition to the variability observed in the clinical penetrance of distinct HCM mutations, there is a great deal of variability in the phenotypes of patients with the same exact mutation. This is likely due to variation in genetic background and the confounding effects of modifier genes. Clinical findings in familial HCM patients show hundreds of causative mutations in the β-myosin protein, and the mutations R453C and R403Q are associated with severe HCM phenotypes in both adults and children (Epstein, Cohn, Cyran, & Fananapazir, 1992; Kaski et al., 2009). The biochemical and systemic characteristics of these mutations have been studied by several groups to unravel the molecular and cellular underpinnings of HCM (Moore, Leinwand, & Warshaw, 2012). However, the proximal effects of these mutations in the cell are unknown. Understanding the mechanism by which mutations R403Q and R453C cause a dangerous disease can allow drug developers to design potent therapeutics. Currently, there are only symptom-alleviating treatments for HCM and the high mortality rates and severe symptoms make developing such treatments a high priority.

HCM is associated cellular- and organ-level remodeling (Berk, Fujiwara, & Lehoux, 2007; Harvey & Leinwand, 2011; Machackova, Barta, & Dhalla, 2006). Most studies probe this pathology using standard featureless tissue culture poly styrene (TCPS) surfaces that are orders of magnitude stiffer than the native cellular environment and do not provide the extracellular scaffolding characteristic of the native tissue. However, many studies are now implementing extracellular scaffolding techniques to create a more *in vivo*-like environment. Furthermore, many groups utilize the tunable properties of hydrogels to create a user-defined extracellular matrix and stiffness. Poly(ethylene) glycol (PEG) is well-known for its biocompatibility and for the synthesis of hydrogel culture scaffolds. Previous work has demonstrated significant cellular adaptations and responses to the stiffness and topography of 2D hydrogels (Camci-unal, Annabi, Dokmeci, Liao, & Khademhosseini, 2014; Duval et al., 2017a; Stout, Yoo, Santiago-, & Webster, 2012). Novel techniques in creating a 3D culture system has allowed researchers to study disease environments (Lewis et al., 2018). Cells respond to extracellular cues such as mechanical stimuli and prefer to inhabit certain environments. For example, cardiac myocytes prefer a 2D plane compared to a 3D suspension (Duval et al., 2017a). These conclusions merit efforts by researchers to customize their cell culture systems based on their cell type of interest. Due to the vast molecular, functional, and structural changes that cardiomyocytes undergo in a 2D culture system, characterizing a 3D culture system may provide an ideal system to study disease on the cellular level.

2. Background

2.1 Hypertrophic cardiomyopathy disease progression

The sarcomere is the basic functional unit a muscle cell. It is present in striated muscle including skeletal and cardiac muscles. It is comprised of about 30-40 proteins that have essential roles in the muscle contraction cycle. There are over 300 HCM-causing genetic mutations that are made up by mutations from each protein in the sarcomere (Watkins et al., 1992). However, this distribution is not balanced. Myosin binding protein C is crucial for sarcomeric organization and cardiac function. It is responsible for about 40% of these mutations (Maron et al., 2001; Schlossarek, Mearini, & Carrier, 2011). In addition, about 30% of the mutations are in a protein called myosin. Myosin binding protein C and myosin are responsible for the majority of the mutations, but myosin is more heavily studied due to its mechanical and biophysical properties.

Myosin is a large, ATP-driven motor protein. It is present in all cells due its involvement in the cellular motility processes, but “conventional” myosin refers to the type of myosin that aggregates into a thick filament within the sarcomere. The thick filament works in conjunction with the thin filament, primarily composed of an actin double helix, to slide past one another. The sliding of the thick and thin filaments, driven by energy, is the process of muscle contraction called the cross-bridge cycle (Brenner, 1986). A review of the biochemical and biophysical properties of cardiomyopathy mutations have been published by Moore et al. In summary, R4303Q and R453C in HCM are gain-of-function mutations and displays and increase in contractile kinetics of the β-myosin motor (Moore et al., 2012). The cellular and organismal consequences of these two mutations are yet to be elucidated, but it is an interest of many groups because of the lack of personalized or curative interventions for patients with HCM.

2.2 Polyethylene glycol (PEG) hydrogels in 2D and 3D culture

HCM is associated with drastic morphological changes such as cellular hypertrophy and severe fibrosis (Popović et al., 2008; Tanaka et al., 1986). Fibrosis is the formation of excess connective tissue in an organ or tissue as a result of disease or injury. Cardiac fibrosis causes stiffening of the heart muscle and can severely impair function because it is irreversible and forms a scar. The interplay between fibrosis and the cardiac myocyte can induce a variety of pathological responses on the cellular level which often leads to functional changes for the whole organ. Most studies probe this pathology using featureless cell culture surfaces that are orders of magnitude stiffer than the native cellular environment. Many bioengineering groups work to address this discrepancy by developing new cell culture methods and materials that include dimensionality and more physiologic substrates (Benton, Fairbanks, & Anseth, 2009; Deforest, Sims, & Anseth, 2010; Mabry, Lawrence, & Anseth, 2015; Shin et al., 2013).

Hydrogels attempt to address the gap in traditional cell culture methods employing glass substrates by providing a simplified recapitulation of the intricate native tissue (Duval et al., 2017b). Hydrogels are gel-like substances that are formed from synthetic polymers. These polymers can crosslink with biological molecules native to the extracellular environment and provide an ideal platform for cell adherence. New chemistries were recently discovered for hydrogel synthesis that are advancing the tunability and application of this cell culture system (Deforest et al., 2010). Implementing this improvement in cell culture is necessary because human tissue dynamics are complex and are pivotal in dictating cellular function but current methods lack these dynamics. Recent work culturing cells on dynamic hydrogels, compared to traditional culture platforms as a control, show that cells on hydrogels display phenotypes and function similar to that seen *in vivo*. For example, valvular interstitial cells were cultured in a 3D hydrogel system to allow researchers to elucidate the cellular response due to 3D mechanical

cues (Mabry et al., 2015) and similar work has been done using induced pluripotent stem cells (Yang, Tibbitt, Basta, & Anseth, 2014).The 3D hydrogel as a culture platform provided the resources for researchers to ask questions that traditional 2D culture surfaces would not permit. Also, the stiffness of the 3D hydrogel can be specified and measured using a rheometer.

2.3 Cellular responses to matrix stiffness and topography

In heart disease, the traditional model system for cell-based studies are primary cells isolated from animals (Peter, Bjerke, & Leinwand, 2016). The protocols for isolating primary cells have been optimized over many years and has become a straightforward technique. Leading investigators in heart disease are striving to use newer and more advanced systems to study disease because it may provide novel insights in understanding disease mechanisms. Alternative and engineered matrices bridge the gap between glass culture substrates and *in vivo* animal models. This is appealing to researchers aiming to model physiological or pathological states. Peter et al. suggest that even though engineered matrices are currently not widely implemented in cell studies, there is a major thrust in cardiac biology to do so because of the potential advantage in understanding biological phenomena.

Previous work has been done in the lab investigating the responses of cardiac myocytes on soft (healthy) and stiff (disease) hydrogel platforms and with various topographies (Figure 1).

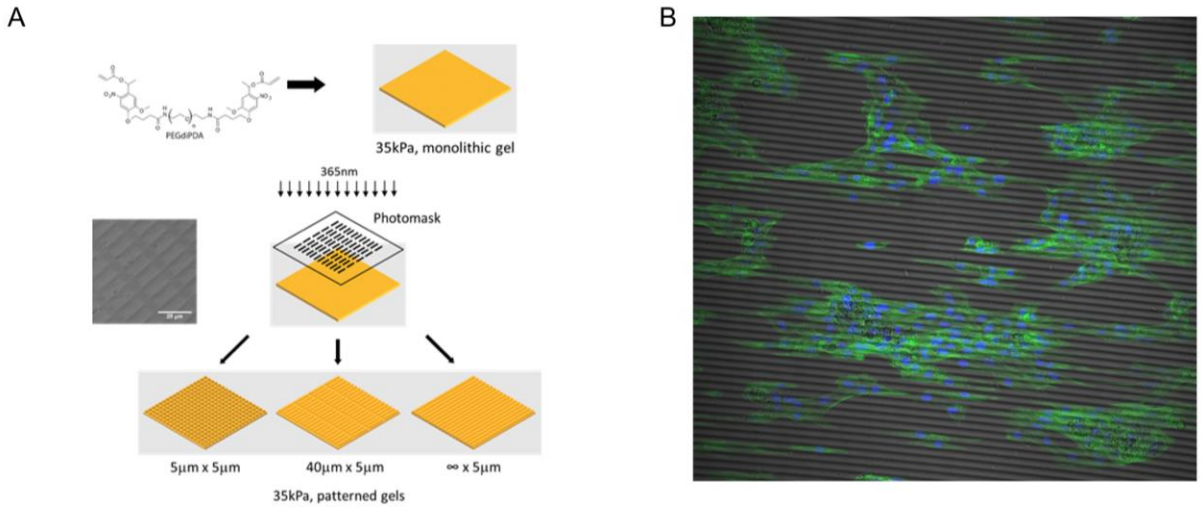

Figure 1: **Neonatal myocytes respond synergistically to substrate stiffness and topography.** a) fabrication of a 2D photodegradable hydrogel in previous work varying substrate stiffness and topography b) NRVMs seeded on a channel patterned 10 kPa hydrogel stained with ActinGreen, and DAPI (adapted from Wan et al., submitted for publication).

Briefly, micropatterned substrates were generated using a photodegradable hydrogel chemistry. The soft gels were a stiffness of 10 kPa and the stiff gels were a stiffness of 35 kPa according to Young's modulus. These stiffness aimed to model healthy and states of the native neonatal rat myocardium (Engler et al., 2008; Majkut et al., 2013). Primary neonatal rat ventricular myocytes (NRVMs) were cultured on smooth, 5μm x 5μm, 10μm x 5μm, 20μm x 5μm, 40μm x 5μm and 5μm wide channels corresponding to aspect ratios of 1:1, 2:1, 4:1, 8:1 and infinity:1 (∞:1) for both stiffnesses (Figure 1A). NRVMs responded synergistically to the microenvironmental cues based on cellular morphology, gene expression, and contractility readouts (Figure 1B). Notably, NRVM and f-actin alignment was proportional to the pattern aspect ratio, fractional shortening

increased with pattern aspect ratio on soft, but not stiff gels, hydrogel stiffness and patterning attenuated pathological fetal gene expression, and pathological miRNA expression decreased on soft patterned gels. The data collected in this work highlight the importance of cell-matrix interactions in regulating intracellular processes of the cardiomyocyte.

3. Specific Aims

The overall aim of this work is to perform initial characterization of cardiomyocytes expressing myosins with HCM-mutations and to generate a viable 3D culture system for cardiac myocytes. This will provide the foundation to study the effects of genetic mutations in a more physiologically-relevant 3D cell culture model. This aim is broken down by these specific questions:

3.2 Do NRVMs show a more physiological profile when cultured in a soft, 3D environment compared to standard tissue culture plastic?

3.1 What are the functional consequences of HCM mutations in NRVMs?

4. Materials and Methods

4.1 Hydrogel formulation

Hydrogels were polymerized by a UV light initiated free radical-mediated cycloaddition reaction between the ene and MMP peptide. An 8-arm PEG norborene (PEG-Nb, Mw~40,000 Da) crosslinker (final concentration 10 wt%) was synthesized as previously described (Fairbanks, Schwartz, Bowman, & Anseth, 2009; Gould, Darling, & Anseth, 2012). An MMP peptide (KCGPQG↓IWGQCK) was purchased from American Peptide Company, Inc. A final concentration of 7mM for the MMP peptide was tethered onto the PEG arms to allow for cell cleavage. 1mM integrin-binding peptide (CRGDs) was also tethered onto the PEG arms (American Peptide Company Inc.). 0.05 wt% lithium phenyl-2,4,6-trimethylbenzoylphosphinate (LAP) that is UV light sensitive was included into the solution to allow reaction to occur. The gel precursor solution (0.75:1 MMP: ene ratio) was buffered to a pH of 7.0 using NaOH, briefly vortexed, and 17uL was pipetted between a SigmaCote (Sigma-Aldrich) siliconized glass slide and a thiol-functionalized 12mm glass coverslip. After exposure to UV light for 3 minutes, the final hydrogel was polymerized and covalently linked to the coverslip. The hydrogel was immersed in phosphate buffered saline (PBS), separated from the glass slide and stored in PBS at 37°C to allow for swelling until use (Figure 2). Rheology of the bottom gel and the sandwich gel was performed using a 1% strain and frequency. Outputs were in storage modulus and then converted to Young's modulus to assess hydrogel stiffness.

4.2 Primary cell isolation and culture

All animal protocols were approved by the University of Colorado Boulder Institutional Animal Care and Use Committee (IACUC). Neonatal rat ventricular myocytes were isolated according to previously published procedures (Maass & Buvoli, 2007). All reagents were purchased from Sigma-Aldrich, unless specified. Hearts from 1-3-day old Sprague-Dawley rats were excised and the ventricles were isolated. The ventricles were minced using scissors and digested in trypsin. Isolated cells were then pre-plated for 2 hours. NRVMs are then collected and counted in a suspension using a hemocytometer. Primary cell isolated were then seeded ~50,000 cells/cm2 on laminin coated hydrogel samples or on glass coverslips in standard tissue culture polystyrene (TCPS) plates (VWR). The first 24 hours of culture are in growth media

containing Minimum Essential Medium (MEM) (Life Technologies) with Hank's salts (Gibco), 5 vol% calf serum, 50U/mL penicillin, 2µg/mL Vitamin B-12, and 30nM bromodeoxyuridine (BrdU). After 24 hours, the cells were washed in a rinse media and continued to be cultured in a serum-free (SF) media consisting of MEM, 10µg/mL insulin, 10µg/mL transferrin, 0.1 wt/vol% bovine serum albumen (BSA), 50U/mL penicillin, 2µg/mL Vitamin B-12, 30nM BruU, and 10 vol% fetal bovine serum (FBS).

4.3 3D hydrogel encapsulation

Gel precursor solutions previously described in 4.1 was used to sandwich primary myocytes (same final concentrations except for MMP final concentration of 9.5mM). Attached myocytes on the bottom gel had media aspirated off in order to pipette a 0.25 ratio (2mM) of MMP for 5 minutes. 17 µL of pH 7.0 top gel precursor was pipetted in between the bottom gel and a SigmaCote (Sigma-Aldrich) siliconized glass slide. After UV light exposure for 1 minute and 30 seconds, the slide was removed after immersion in PBS. The top gel will crosslink to the bottom gel to 3D encapsulate the primary cells with a final MMP:ene ratio of 1:1.

4.5 Recombinant adenoviral generation and infection

A recombinant adenovirus was generated to express the human αMyHC gene (MYH6). Three separate viruses encoding WT, R403Q, and R453C were cloned using a virus provided by the Regnier lab (University of Washington, Seattle). Briefly, the mCMV promoter and polyA sequences were cloned from viral DNA using PCR and inserted into the cloning vector pShuttle (New England Biosciences). Mutagenesis PCR was performed to create the R403Q and R453C missense mutations in the MYH6 gene. The mCMV promoter, MYH6 (WT, RQ, RC), and the polyA tail was then cloned into pShuttle (Addgene) using restriction digests. These plasmids were purified and sequenced. Correct sequences were then homologously recombined with the adenoviral vector pAdEasy-1 (Addgene) in RecA+ cells. The pAdEasy-1 vector with the gene of interest was digested with a PacI enzyme and a phenol-chloroform extraction with an ethanol precipitation was performed to purify the DNA. The purified adenoviral vector with MYH6 (WT, RQ, RC) was transfected into HEK 293 cells for a serial propagation of the adenoviruses. The virus preparations were purified by banding on CsCl gradients. The mature viral bands were extracted and the viral titer was determined through plaque assays as previously described (Langer, Ghafoori, Byrd, & Leinwand, 2002).

The viral multiplicity of infection (MOI) was chosen based on the highest number of infected cells with the least amount toxicity. MOIs of 10, 20, and 40 were tested, and the MOI of 20 fit the desired criteria. NRVMs were infected with the adenoviruses for 24 hours in SF media post a 24 hour plating period in growth media. Then the virus containing media was washed and the NRVMs were cultured for an additional 24 hours. All cellular and molecular assays were conducted after 48 hours of virus contact.

4.6 Immunostaining

For the HCM studies, cells were fixed in 4% paraformaldehyde (PFA) (Electron Microscopy Sciences) for 5 minutes. The cells were washed in PBS at each step. After fixation, the samples were permeabilized in 0.1% TritonX-100 (Fisher) for 3 minutes and blocked in 3% BSA. A primary mouse-anti DYKDDDDK (FLAG) tag antibody (Cell Signaling Technology) was pipetted onto the samples and incubated for 1 hour, followed by a 30-min incubation with the Alexa Fluor 488 fluorophore anti-mouse secondary probe (Life Technologies). 4',6-diamidino-2-phenylindole, DAPI (Life Technologies) and ActinRed™ 555 ReadyProbes™ Reagent (Thermo Fisher Scientific) according to manufacturer's instructions. The primary antibody was used at a 1:1600 dilution and the secondary antibody was used at a 1:1000 dilution.

For the 3D hydrogel samples, cells were fixed in formalin for 30 minutes, permeabilized with PBST, blocked with 1% BSA, incubated with a primary monoclonal anti-α-Actinin (Sarcomeric) antibody produced in mouse (Sigma) overnight in 4°C, then incubated with secondary antibody overnight. 4',6-diamidino-2-phenylindole, DAPI (Life Technologies) and ActinRed™ 555 ReadyProbes™ Reagent (Thermo Fisher Scientific) according to manufacturer's instructions. The primary antibody was used at a 1:200 dilution and the secondary antibody was used at a 1:1000 dilution.

4.7 Fractional shortening

Videos of live spontaneously contractive live cells were collected through a 40x objective (N.A. XX) on the Nikon N-STORM super resolution microscope equipped with high-speed EMCCD cameras. The cells were stained with 2μM CellTracker™ Red CMTPX Dye (Thermo Fisher Scientific) diluted in SF media (incubated for 30 minutes). During the imaging, the cells were maintained in warm Tyrode's solution. The videos were segmented for single cells and then analyzed with a custom Matlab (MathWorks, Natick, MA) script. The output fractional shortening (FS) measurements were calculated according to

$$FS = \frac{L_D - L_S}{L_D} \times 100$$

L_S is the major axis of the maximally contracted cell where as L_D is the major axis of a fully relaxed cell. Each frame was thresholded to identify the single cell and the area was calculated using a built-in Matlab function, regionprops.

4.8 Hydrogel erosion

3D hydrogels were digested with collagenase type 2 (Worthington Biochemical) for 30-40 minutes and the TCPS controls were treated with trypsin (Worthington Biochemical) for 5 minutes. The suspension of cells and gel components were centrifuged at 1000 RPM for 5 minutes to remove gel components and to pellet the cells. The pellet was then resuspended in for washing steps and repelleted for storage at -20 degrees celcius.

4.9 RNA isolation and Quantitative PCR

For the hydrogel studies, RNA was isolated by manufacturer's instructions (RNeasy Minikit, Qiagen) after fixation. RNA concentration and quality were measured and assessed using a spectrophotometer (Nanodrop 1000, Thermo Scientific). In order to perform quantitative PCR (qPCR), cDNA was synthesized from mRNA by reverse-transcriptase PCR (RT-PCR) per manufacturer's instructions using (SuperScript III, First-stand synthesis kit, Invitrogen). Random hexamers were the primers of choice. qPCR master mix reactions were prepared including forward and reverse primers (420nM each) and SYBR green (Applied Biosystems) with a final volume of 10μL (Table 1).

The master mix and samples were loaded into a thermal cycler (Bio-Rad) compatible 96-well plate and run through a program per SYBR green's instructions. A reference gene was determined, and the relative quantification concluded after normalization.

5. Results

5.1 in situ rheology reveals the 3D hydrogel stiffness to be around 30 and 40 kPa in Young's modulus

Biological substrates, blood, brain, muscle and collagenous bone range in stiffnesses of 1 to 100 kPa (Figure 3A). Standard tissue culture substrates, plastic and glass, are orders of magnitude stiffer and out of the range of biological elasticity. Rheological measurements show that the bottom hydrogel (1:1 thiol:ene) stiffness to be around 30 kPa in Young's modulus (Figure 3B). With the additional 0.75 MMP and the top gel layer added, the hydrogel stiffness increased slightly to be around 40 kPa, although this was non-significant (Figure 3B). The hydrogels provide a culture substrate stiffness slightly stiffer than muscle; however it is within the physiological range compared to plastic or glass.

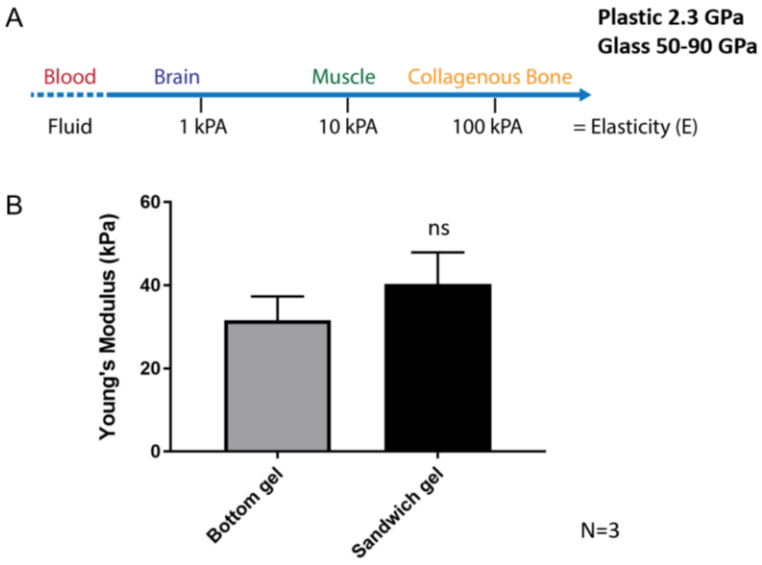

Figure 3: **3D sandwich gel characterization.** a) native stiffnesses of biological and culture substrates b) *in situ* rheology of bottom gel and 3D sandwich gel with stiffnesses around 30 kPa and 40 kPa in Young's modulus

5.2 NRVMs are viable in 3D hydrogel culture and display different morphology

NRVMs encapsulated in a 3D hydrogel are viable. This was confirmed by immunostaining with ethidium homodimer (red) to mark the dead cells and calcien AM (green) to mark the live cells. Live/dead fluorescent microscopic images show comparable amounts of live NRVMs in 3D compared to TCPS controls (Figure 4A). The culture technique was improved and practiced to yield an increase number of live NRVMs in 3D (Figure 4B). There is an greater ratio of live:dead cells in both TCPS and 3D culture conditions after optimization. The newer replicate of a higher number of live cells was used for further studies. It is also important to mention that due to the nature of the 3D encapsulation, any cell death that occurred during the culture process will be accounted for in 3D gels and not TCPS. Dead cells in a TCPS culture detach from the plate and are washed off whereas in a gel, they remain. This can negatively alter live:dead ratio of NRVMs cultured in 3D.

Interestingly, there was a stark difference in cell morphology that was followed up with automated analysis. There is a significant decrease in cell size of NRVMs cultured in 3D compared to on TCPS (Figure 4C). However, it is important to note that this automated analysis was performed on image planes and do not represent a volumetric measurements. This conclusion supports the hypothesis that in a 3D environment, cells are not forced to take a flat shape and can take a more 3D shape.

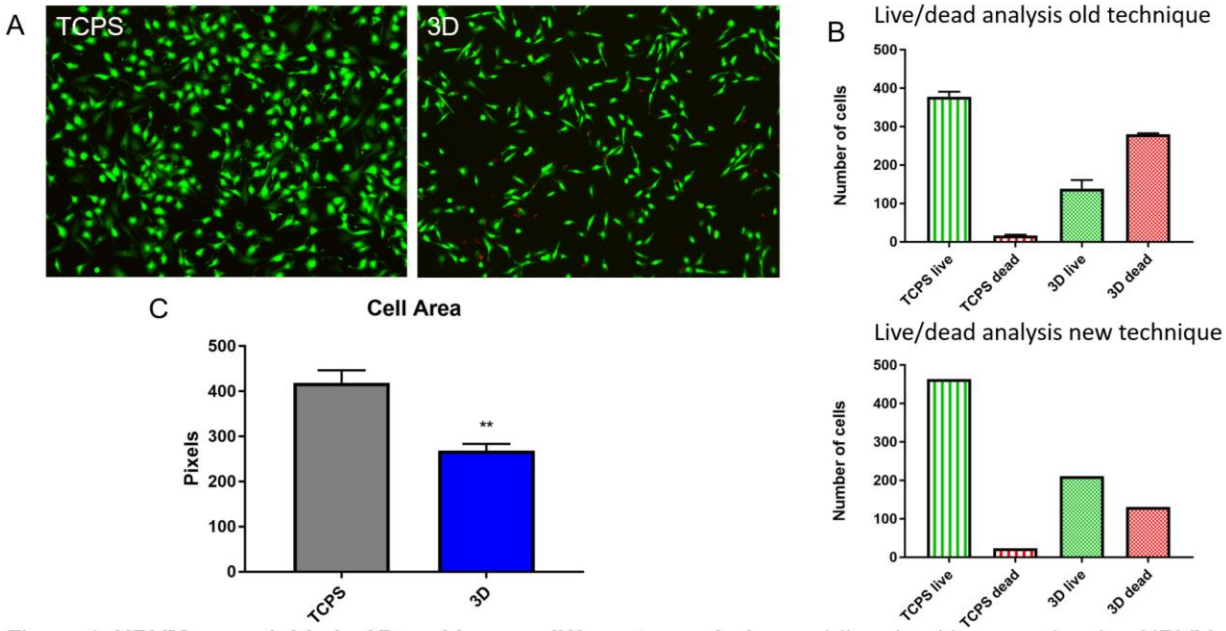

Figure 4: **NRVMs are viable in 3D and have a different morphology.** a) live-dead images showing NRVMs on TCPS and in 3D b) encapsulation and cell culture technique improved by live-dead analysis, green representing calcien AM positive cells and red showing ethidium homodimer positive cells c) difference in cell size of NRVMs on TCPS vs. in 3D

5.3 NRVMs infected HCM adenoviruses show expression and incorporation

The recombinant adenoviruses used to express HCM-mutant α-myosin proteins in NRVMs was generated by DNA cloning. The gene construct is shown in Figure 5A. The human α-myosin gene sequence was cloned into a cloning vector. Then the mCMV promoter, polyA tail, and FLAG-tag (DYKDDDDK) were added in. Three constructs were created for the wild-type sequence, the R403Q mutation, and the R453C mutation. Each construct was then cloned into a viral plasmid. The WT, RQ, and RC viruses were propagated and the viral titers were determined by plaque-counting assays. Using a multiplicity of infection of 40, the expression of the HCM myosins were assessed.

By 24 hours, NRVMs showed a high expression of the FLAG-tagged α-myosin proteins (Figure 5B). This was confirmed by immuostaining with DAPI, Actin Red, and AF488 anti FLAG. A 20x scan was stiched together to confirm high infectivity and expression. Higher resolution and magnification images images were taken to assess incorporation of the FLAG-tagged myosin within the sarcomeric structure. Recycling of endogenous myosin for the FLAG-tagged myosin was confirmed in these images (Figure 5C).

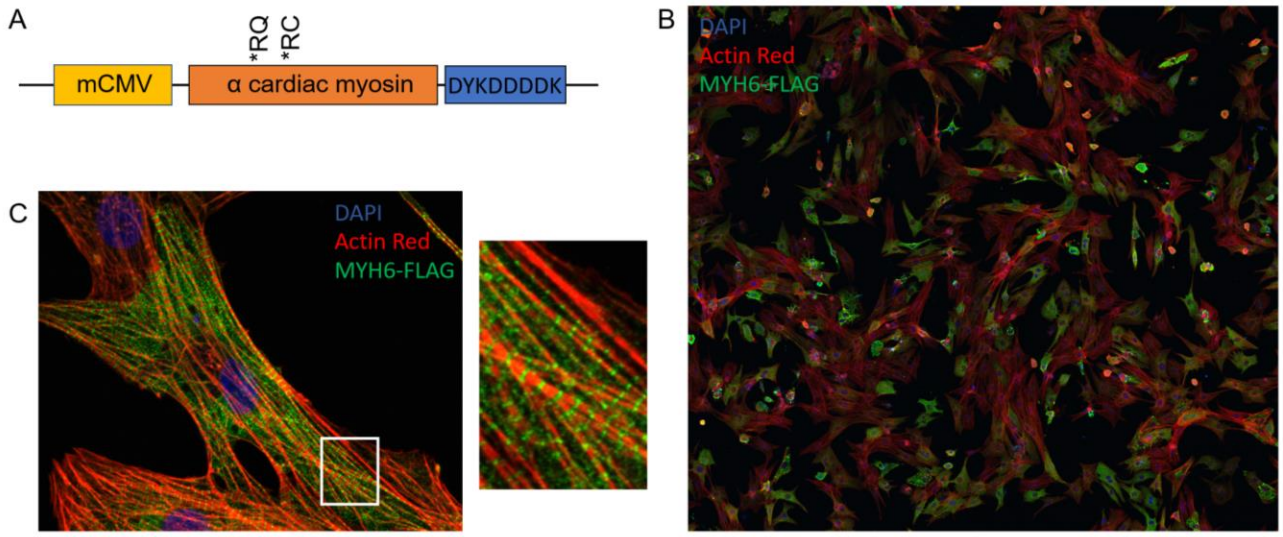

Figure 5: **Expression and incorporation of adenoviral α-myosin.** a) α-myosin gene construct is driven by the mCMV promoter, FLAG-tagged (DYKDDDK), and the two mutations of interest are R403Q and R453C b) high infectivity and expression of the adenoviral introduced α-myosin (green is MYH6-FLAG, Actin Red, and DAPI) c) incorporation of the FLAG-tagged α-myosin in NRVMs

5.4 Expression of α-myosin was measured by western blot and multiplicity of infection equalized

The protein content of α-myosin-FLAG was measured by western blotting (Figure 6A). MYH6-FLAG and actin were probed and MYH6-FLAG levels were normalized to actin. The multiplicity of infections were adjusted appropriately to yeild equalized expression in the WT, R403Q, and R453C groups (Figure 6B). This allowed for the functional and molecular analysis to be based on the effects of the mutations versus levels of mutant protein.

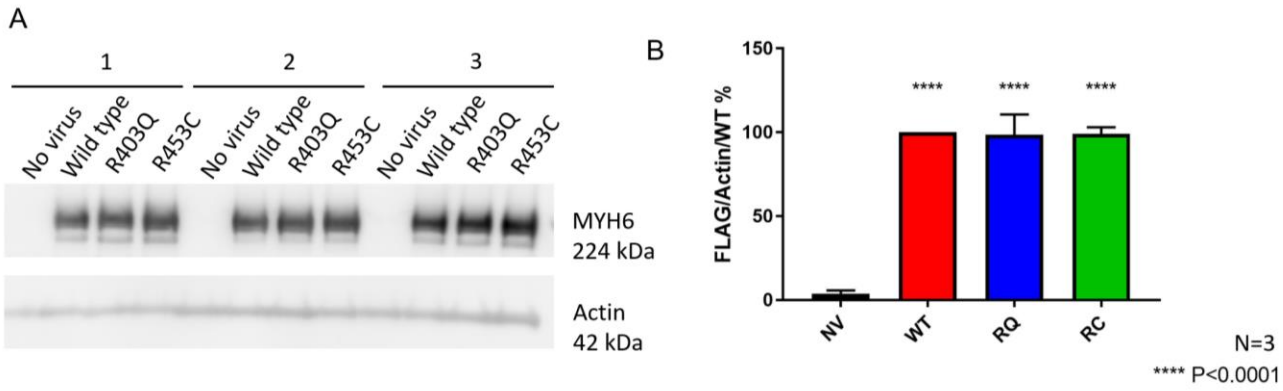

Figure 6: **Equalizing expression of virally-introduced myosin.** a) Western blot for three biological replicates probing for MYH6 (224 kDa) and normalized to actin (42 kDa) b) Quantification of western blot analysis normalized to actin and WT by percent (NV was the control resulting in no viral protein expression)

5.5 Preliminary data on HCM cellular contractile kinetics

Fractional shortening is a measure of contractile function. 15 second videos of single CellTracker Red stained cells were recorded and inputed into a custom MATLAB program (Figure 7B). The program drew an elipse around the single cell and recorded changes in major axis length over time. Preliminary results show an increase in fractional shortening for R403Q compared to the wildtype group (Figure 7A). Since the cells spontaneously contract, an electrical stimulus was not applied in these data. However, non-uniform and uniform contraction in some on the NRVMs were observed. Non-uniform contracting cells displayed a contraction on different axses in the cell while uniform contrating cells contracted on a single cell axis. An exclusion criteria was contructed based on this observation and it also excluded cells that did not contract 10 or more consecutive beats.

After collecting the fractional shortening measurements, the NRVMs were fixed and immunostained to validate the expression and incorporation of MYH6-FLAG in the HCM groups (Figure 7B). The left panel of Figure 7C shows the no virus group with only CellTracker Red and DAPI staining. The right panel of Figure 7C shows the WT HCM NRVMs with CellTracker Red, DAPI, and MYH6-FLAG. Since the initial cell selection is unbiased because all of the NRVMs are stained with only CellTracker red, positive immunostaining for MYH6-FLAG ensured that the differences seen are due to the expression of WT or RQ mutant or RC mutant myosin.

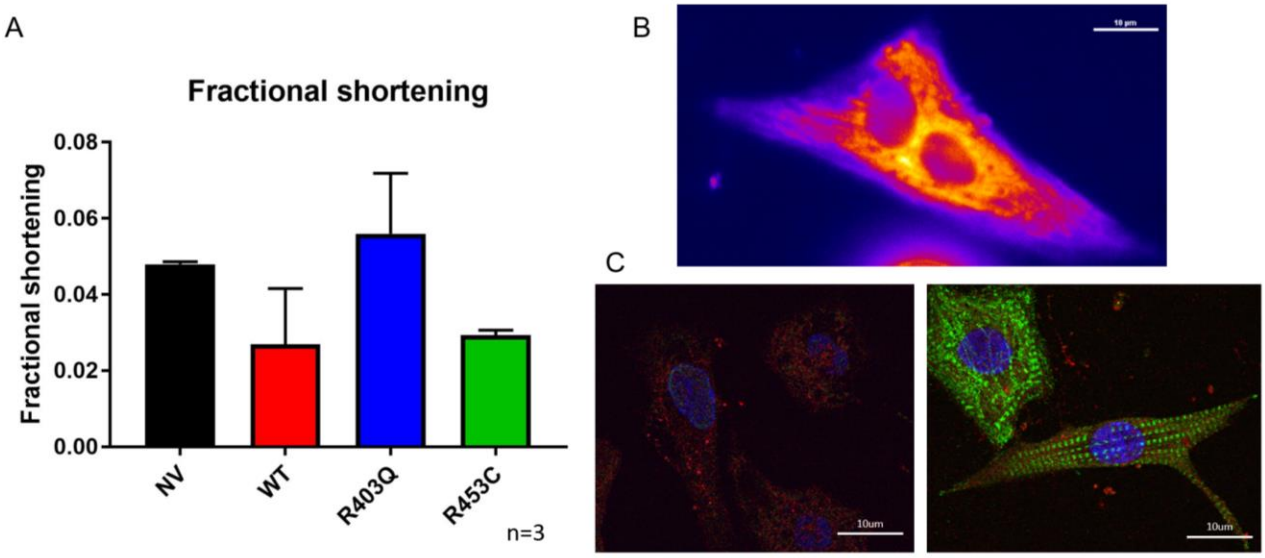

Figure 7: **Preliminary data on contractile kinetics of NRVMs with HCM mutations.** a) Fractional shortening measurements of NRVMs showing a trend of increased contractility in NRVMs with mutation R403Q b) Sample video used in MATLAB analysis c) Post-data collection immunostaining to validate analysis on infected and non-infected cells

6. Discussion and Future Directions

6.1 Implementing a 3D cell culture system can potentially provide a more appropriate disease model

This novel 3D cell culture system presented in this work more accurately mimics the native tissue with stiffness and matrix tunability. NRVMs are viable and display a physiological response in a 3D hydrogel compared to NRVMs cultured on TCPS. Initial characterization of NRVMs in 3D revealed that NRVMs process and respond to microenvironmental cues such as

mechanical stimuli. There was a comparable number of live NRVMs in 3D to TCPS. Cells in 3D were encapsulated and any dead cells remaining cannot escape compared to the dead cells that are washed off for the TCPS condition. This alteration in live:dead cell ratios in gels compared to TCPS were kept in mind and with the resulting ratio being greater than 1 in the repeated replicates, it can be concluded that this culture system is viable. *In situ* rheology demonstrated that the elasticity of the bottom and top layer were not significant although the sandwich gel trended to be a few kPa stiffer. The stiffness of the hydrogels are within the range of muscle stiffness of 10 kPa compared to plastic of about 2.3 GPa.

Notably, there was a significant difference in cell size of NRVMs in 3D compared to TCPS. This can be partially explained by gravitational forces acting on the cells on TCPS causing the cells to expand and flatten. Cells in 3D are not forced to spread and may adopt a more physiologicaly favorable shape. Further investigation into the molecular cues directing cell shape is needed. Neonatal cardiomyocytes possess a star-like shape whereas adult cardiomyocytes have matured into a brick-like organized shape. If culturing NRVMs in 3D allow for the maturation into an adult cellular phenotype, this culture method can address the gap in knowledge about the factors driving this shift.

Functional and molecular readouts such as contractility and gene expression for NRVMs cultured in 3D need to analyzed to assess cell health; however, these readouts were beyond the scope of this work and the live/dead cell staining was enough to suggest that researchers studying disease should consider the conditions that the cells are in. Based on this work, cell culture conditions can impact the baseline of cell health that disease models are compared to.

6.2 Molecular and cellular characteristics of HCM myosins leading to the development of therapeutics

The recombinant adenoviruses generated using DNA cloning techniques to express mutant myosins intracellularly were validated in these studies through expression and incorporation analyses. Based on these data, the acute effects of HCM mutations observed in this study are plausible. On the level of the organ, there is an increase in left ventricular size due to cellular hypertrophy. There was an increase in cell area and aspect ratio for cells that expressed and incorporated the R453C HCM mutant myosin and both R403Q and R453C compared to the control; repectively (Figure S1A and S1B). Based on these preliminary results, expressing HCM-mutatn myosins can cause HCM phenotypes. Single-cell fractional shortening measurements yielded an increase in HCM myocytes compared to WT and TCPS controls indicating that the incorporation of a mutant myosin causes a whole-cell effect of hypercontraction. This aligns with previous biophysical work analyzing the effects of the myosin motor (Moore et al., 2012). Preliminary gene expression profiles of HCM myocytes compared to controls showed an activation of pathologic genes such as ANF and BNP (Figure S2). It is interesting to note that even though the viral protein expressed was a α-myosin, the myocyte may be recycling the α-myosin molecule at a much faster rate than myocytes without the HCM mutation. Therefore, the mutation may affect other cell signaling pathways in protein degradation in addition to cell function.

These preliminary characteristics of NRVMs infected with HCM-myosin adenoviruses suggest that the expression of HCM mutations is sufficient to cause a cellular disease phenotype. Having a cellular model of HCM can provide a deconvoluted platform for drug discovery. Other groups have begun high-throughput drug screening using small molecule activators and iPSC models of HCM (Carlson et al., 2013; Reid et al., 2016). However, myocytes with mutation specific myosins present in the cell can provide a more accurate disease model and a higher level of specificity for the development of therapeutics.

6.3 Studying HCM in a 3D cell culture system

Based on these data, future studies should implement a 3D hydrogel culture system in cellular studies. Viral expression and incorporation of HCM mutant myosins on TCPS are sufficient to create a cellular disease phenotype, and NRVMs cultured and infected in 3D should also be able to display a disease phenotype because the viral particles are small enough to penetrate through a gel matrix and reach the cells. NRVMs in 3D display a healthier baseline, so it would be beneficial to study the molecular and cellular consequences of HCM in 3D compared to TCPS because the effects may be amplified or clearer compared to a pre-disposed cell cultured on TCPS.

The idea of using a physiological cell culture system can be extended to human induced pluripotent stem cell (iPSCs) studies of HCM and other diseases for the same reasoning mentioned above. Many groups are supportive this motion because a more accurate representation of a disease leads to better interpretations and development of therapeutics (Bhana et al., 2010; Duval et al., 2017b; Peter et al., 2016).

6.4 Limitations

It is important to note that the translation of this cellular HCM disease model may not be straight forward due to the species discrepancy. Neonata rat cells were used in this study instead of human cells because it is a standard of basic science research due to some species similarities as well as availability and ease-of-use. HCM mutations in myosin in humans are primarily in the β isoform. β-myosin is the dominant isoform in humans whereas the α-myosin is the dominant form in rats. In this study, the human β-myosin mutations were expressed in the α-myosin gene because it is the dominant isoform in rats. Although the data supports that the change in isoform still presents the human HCM phenotypes, further studies in human cells with the mutations in the β-myosin are required to translate these findings into further studies.

The hydrogels used in this experiment do not contain the complex and constant biochemical and mechanical stimuli present in the native tissue. Therefore, this model could be further optimized in specific disease models. For example, in the context of this study, a co-culture of myoctyes and fibroblasts in 3D would aid in creating a model that resembles the native tissue because fibroblasts and myocytes are in constant communication. In this co-culture, the myocytes would be able to respond to cellular signals secreted by the fibroblast in the hydrogel matrix and vice versa. The hydrogel also is a stagnant stiffness. Although the stiffness can be tuned, it is not dynamic. Gel chemistries with photoresponsive hydrogel cross-linkers can soften or stiffen a gel matrix over time which would provide another perspective of optimization.

7. Conclusion

Overall, virally introduced expression of myosin carrying HCM-causing mutations can cause NRVMs to present a disease phenotype and a 3D hydrogel cell culture system was developed to potentially provide a more physiological environment compared to standard culture methods. Morphological, functional, and molecular characterizations showed differences in cells with HCM myosins and WT myosins. NRVMs cultured in a 3D hydrogel displayed a more physiologic profile compared to NRVMs cultured on standard 2D tissue culture platforms. The NRVMs were viable and showed interesting morphological differences suggesting that microenvironmental signals are integrated intracellularly and affect cellular responses. Future studies studying cellular models of disease can be performed in a 3D cell culture environment for a more *in-vivo*-like baseline to compare disease characteristics.

8. Acknowledgements

This work was supported by the American Heart Association Undergraduate Fellowship (16UFEL31660000) for the HCM studies and by the University of Colorado Boulder Undergraduate Research Opportunities Program (Assistantship and Individual Grants).

I would like to thank Dr. Leslie Leinwand and Dr. Kristi Anseth for the special mentorship and support. It has been such an incredible opportunity to work in the Leinwand and Anseth labs over the past four years. Dr. Leinwand and Dr. Anseth are extraordinary investigators and have allowed me to develop a personalized perspective on successful research.

I would like to thank Dr. Pam Harvey for teaching me to think critically about the components of research and for advising my thesis.

Thank you to Dr. Maureen Bjerke, Dr. William Wan, and Dr. Kristen Barthel for mentoring me at the bench and helping me develop technical skills. Dr. Barthel provided the encouragement to get involved in research and I am forever grateful. Dr. Wan and Dr. Bjerke have invested many hours into my development into an independent scientist which has heavily shaped my career goals.

I would like to thank Tova Christensen for inspiration and logistical work for the engineering for the hydrogels.

I would like to thank Jessica Hall for providing support and inspiration for this project. This could not be possible without her physical help and emotional support.

I would like to thank Ann Robinson and Dr. Angela Peter for the NRVM work. They performed all the primary NRVM/NRVF isolations and the media for cell culture.

Finally, I would like to thank Dr. Levente Szentkirályi for guidance in the writing preparation of this thesis and the final revisions of this work.

9. References

Benton, J. A., Fairbanks, B. D., & Anseth, K. S. (2009). Characterization of valvular interstitial cell function in three dimensional matrix metalloproteinase degradable PEG hydrogels. *Biomaterials*, *30*(34), 6593–6603. https://doi.org/10.1016/j.biomaterials.2009.08.031

Berk, B. C., Fujiwara, K., & Lehoux, S. (2007). ECM remodeling in hypertensive heart disease. *The Journal of Clinical Investigation*, *117*(3), 568–575. https://doi.org/10.1172/JCI31044

Bhana, B., Iyer, R. K., Chen, W. L. K., Zhao, R., Sider, K. L., Likhitpanichkul, M., … Radisic, M. (2010). Influence of substrate stiffness on the phenotype of heart cells. *Biotechnology and Bioengineering*, *105*(6), 1148–1160. https://doi.org/10.1002/bit.22647

Brenner, B. (1986). The cross-bridge cycle in muscle. Mechanical, biochemical, and structural studies on single skinned rabbit psoas fibers to characterize cross-bridge kinetics in muscle for correlation with the actomyosin-ATPase in solution BT - Controversial issues in ca. In R. Jacob (Ed.) (pp. 1–15). Heidelberg: Steinkopff. https://doi.org/10.1007/978-3-662-11374-5_1

Camci-unal, G., Annabi, N., Dokmeci, M. R., Liao, R., & Khademhosseini, A. (2014). Hydrogels for cardiac tissue engineering, (October 2013). https://doi.org/10.1038/am.2014.19

Carlson, C., Koonce, C., Aoyama, N., Einhorn, S., Fiene, S., Thompson, A., … Kattman, S. (2013). Phenotypic Screening with Human iPS Cell–Derived Cardiomyocytes: HTS-Compatible Assays for Interrogating Cardiac Hypertrophy. *Journal of Biomolecular Screening*, *18*(10), 1203–1211. https://doi.org/10.1177/1087057113500812

Deforest, C. A., Sims, E. A., & Anseth, K. S. (2010). Peptide-functionalized click hydrogels with independently tunable mechanics and chemical functionality for 3D cell culture. *Chemistry of Materials*, *22*(16), 4783–4790. https://doi.org/10.1021/cm101391y

Duval, K., Grover, H., Han, L.-H., Mou, Y., Pegoraro, A. F., Fredberg, J., & Chen, Z. (2017a). Modeling Physiological Events in 2D vs. 3D Cell Culture. *Physiology*, *32*(4), 266–277. https://doi.org/10.1152/physiol.00036.2016

Duval, K., Grover, H., Han, L.-H., Mou, Y., Pegoraro, A. F., Fredberg, J., & Chen, Z. (2017b). Modeling Physiological Events in 2D vs. 3D Cell Culture. *Physiology*, *32*(4), 266 LP-277. Retrieved from http://physiologyonline.physiology.org/content/32/4/266.abstract

Engler, A. J., Carag-Krieger, C., Johnson, C. P., Raab, M., Tang, H.-Y., Speicher, D. W., … Discher, D. E. (2008). Embryonic cardiomyocytes beat best on a matrix with heart-like elasticity: scar-like rigidity inhibits beating. *Journal of Cell Science*, *121*(22), 3794 LP-3802. Retrieved from http://jcs.biologists.org/content/121/22/3794.abstract

Epstein, N. D., Cohn, G. M., Cyran, F., & Fananapazir, L. (1992). Differences in clinical expression of hypertrophic cardiomyopathy associated with two distinct mutations in the beta-myosin heavy chain gene. A 908Leu----Val mutation and a 403Arg----Gln mutation. *Circulation*, *86*(2), 345–352. https://doi.org/10.1161/01.CIR.86.2.345

Fairbanks, B. D., Schwartz, M. P., Bowman, C. N., & Anseth, K. S. (2009). Photoinitiated polymerization of PEG-diacrylate with lithium phenyl-2,4,6-trimethylbenzoylphosphinate: polymerization rate and cytocompatibility. *Biomaterials*, *30*(35), 6702–6707. https://doi.org/https://doi.org/10.1016/j.biomaterials.2009.08.055

Gould, S. T., Darling, N. J., & Anseth, K. S. (2012). Small peptide functionalized thiol–ene hydrogels as culture substrates for understanding valvular interstitial cell activation and de novo tissue deposition. *Acta Biomaterialia*, *8*(9), 3201–3209. https://doi.org/https://doi.org/10.1016/j.actbio.2012.05.009

Harvey, P. A., & Leinwand, L. A. (2011). Cellular mechanisms of cardiomyopathy. *The Journal of Cell Biology*, *194*(3), 355 LP-365. Retrieved from http://jcb.rupress.org/content/194/3/355.abstract

Kaski, J. P., Syrris, P., Esteban, M. T. T., Jenkins, S., Pantazis, A., Deanfield, J. E., … Elliott, P. M. (2009). Prevalence of Sarcomere Protein Gene Mutations in Preadolescent Children With Hypertrophic Cardiomyopathy. *Circulation: Cardiovascular Genetics*, *2*(5), 436–441. https://doi.org/10.1161/CIRCGENETICS.108.821314

Langer, S. J., Ghafoori, A. P., Byrd, M., & Leinwand, L. (2002). A genetic screen identifies novel non-compatible loxP sites. *Nucleic Acids Research*, *30*(14), 3067–3077. Retrieved from http://dx.doi.org/10.1093/nar/gkf421

Lewis, K. J. R., Hall, J. K., Kiyotake, E. A., Christensen, T., Balasubramaniam, V., & Anseth, K. S. (2018). Epithelial-mesenchymal crosstalk influences cellular behavior in a 3D alveolus-fibroblast model system. *Biomaterials*, *155*(Supplement C), 124–134. https://doi.org/https://doi.org/10.1016/j.biomaterials.2017.11.008

Maass, A. H., & Buvoli, M. (2007). Cardiomyocyte Preparation, Culture, and Gene Transfer BT - Cardiac Gene Expression: Methods and Protocols. In J. Zhang & G. Rokosh (Eds.) (pp. 321–330). Totowa, NJ: Humana Press. https://doi.org/10.1007/978-1-59745-030-0_18

Mabry, K. M., Lawrence, R. L., & Anseth, K. S. (2015). Dynamic stiffening of poly(ethylene glycol)-based hydrogels to direct valvular interstitial cell phenotype in a three-dimensional environment. *Biomaterials*, *49*, 47–56. https://doi.org/10.1016/j.biomaterials.2015.01.047

Machackova, J., Barta, J., & Dhalla, N. S. (2006). Myofibrillar remodelling in cardiac hypertrophy, heart failure and cardiomyopathies. *The Canadian Journal of Cardiology*, *22*(11), 953–968. Retrieved from http://www.ncbi.nlm.nih.gov/pmc/articles/PMC2570240/

Majkut, S., Idema, T., Swift, J., Krieger, C., Liu, A., & Discher, D. E. (2013). Heart-Specific Stiffening in Early Embryos Parallels Matrix and Myosin Expression to Optimize Beating. *Current Biology*, *23*(23), 2434–2439. https://doi.org/https://doi.org/10.1016/j.cub.2013.10.057

Maron, B. J., Niimura, H., Casey, S. A., Soper, M. K., Wright, G. B., Seidman, J. G., & Seidman, C. E. (2001). Development of left ventricular hypertrophy in adults with hypertrophic cardiomyopathy caused by cardiac myosin-binding protein C gene mutations. *Journal of the American College of Cardiology*, *38*(2), 315–321. https://doi.org/https://doi.org/10.1016/S0735-1097(01)01386-9

Moore, J. R., Leinwand, L., & Warshaw, D. M. (2012). Understanding Cardiomyopathy Phenotypes Based on the Functional Impact of Mutations in the Myosin Motor. *Circulation Research*, *111*(3), 375 LP-385. Retrieved from http://circres.ahajournals.org/content/111/3/375.abstract

Morita, H., Rehm, H. L., Menesses, A., McDonough, B., Roberts, A. E., Kucherlapati, R., … Seidman, C. E. (2008). Shared genetic causes of cardiac hypertrophy in children and adults. *The New England Journal of Medicine*, *358*(18), 1899–908. https://doi.org/10.1056/NEJMoa075463

Peter, A. K., Bjerke, M. A., & Leinwand, L. A. (2016). Biology of the cardiac myocyte in heart disease. *Molecular Biology of the Cell* , *27*(14), 2149–2160. https://doi.org/10.1091/mbc.E16-01-0038

Popović, Z. B., Kwon, D. H., Mishra, M., Buakhamsri, A., Greenberg, N. L., Thamilarasan, M., … Desai, M. Y. (2008). Association Between Regional Ventricular Function and Myocardial Fibrosis in Hypertrophic Cardiomyopathy Assessed by Speckle Tracking Echocardiography and Delayed Hyperenhancement Magnetic Resonance Imaging. *Journal of the American Society of Echocardiography*, *21*(12), 1299–1305. https://doi.org/https://doi.org/10.1016/j.echo.2008.09.011

Reid, B. G., Stratton, M. S., Bowers, S., Cavasin, M. A., Demos-Davies, K. M., Susano, I., & McKinsey, T. A. (2016). Discovery of novel small molecule inhibitors of cardiac hypertrophy using high throughput, high content imaging. *Journal of Molecular and Cellular Cardiology*, *97*, 106–113. https://doi.org/10.1016/j.yjmcc.2016.04.015

Richard, P. (2003). Hypertrophic Cardiomyopathy: Distribution of Disease Genes, Spectrum of Mutations, and Implications for a Molecular Diagnosis Strategy. *Circulation*, *107*(17), 2227–2232. https://doi.org/10.1161/01.CIR.0000066323.15244.54

Schlossarek, S., Mearini, G., & Carrier, L. (2011). Cardiac myosin-binding protein C in hypertrophic cardiomyopathy: Mechanisms and therapeutic opportunities. *Journal of*

Molecular and Cellular Cardiology, *50*(4), 613–620. https://doi.org/https://doi.org/10.1016/j.yjmcc.2011.01.014

Seidman, C. E., & Seidman, J. G. (2011). Identifying Sarcomere Gene Mutations in HCM: A Personal History. *Circulation Research*, *108*(6), 10.1161/CIRCRESAHA.110.223834. https://doi.org/10.1161/CIRCRESAHA.110.223834

Shin, S. R., Jung, S. M., Zalabany, M., Kim, K., Zorlutuna, P., Kim, S., … Palacios, T. (2013). Hydrogel Sheets for Engineering Cardiac Constructs and Bioactuators, (3), 2369–2380.

Stout, D. A., Yoo, J., Santiago-, A. N., & Webster, T. J. (2012). Mechanisms of greater cardiomyocyte functions on conductive nanoengineered composites for cardiovascular application, 5653–5669.

Tanaka, M., Fujiwara, H., Onodera, T., Wu, D. J., Hamashima, Y., & Kawai, C. (1986). Quantitative analysis of myocardial fibrosis in normals, hypertensive hearts, and hypertrophic cardiomyopathy. *British Heart Journal*, *55*(6), 575 LP-581. Retrieved from http://heart.bmj.com/content/55/6/575.abstract

Watkins, H., Rosenzweig, A., Hwang, D.-S., Levi, T., McKenna, W., Seidman, C. E., & Seidman, J. G. (1992). Characteristics and Prognostic Implications of Myosin Missense Mutations in Familial Hypertrophic Cardiomyopathy. *New England Journal of Medicine*, *326*(17), 1108–1114. https://doi.org/10.1056/NEJM199204233261703

Yang, C., Tibbitt, M. W., Basta, L., & Anseth, K. S. (2014). Mechanical memory and dosing influence stem cell fate. *Nat Mater*, *13*(6), 645–652. Retrieved from http://dx.doi.org/10.1038/nmat3889

10. Supplemental Material

Gene	Sequence
ANF	AAATCCCGTATACAGTGCGG
	GGAGGCATGACCTCATCTTC
BNP	CCAGAACAATCCACGATGC
	TCGAAGTCTCTCCTGGATCC
COL1A1	AGGTCGCACTGGCGATAG
	GGCCACCATCTTGAGACTTC
MYH6 (alpha)	TGCAGAAGAAACTGAAGGAAAA
	GCTCGGCCTCTAGCTCCT
MYH7 (beta)	CTCCAGAAGAGAAGAACTCC
	CCACCTGCTGGACATTCTGC
18s	GCCGCTAGAGGTGAAATTCTTG
	CTTTCGCTCTGGTCCGTCTT

Table S1: **Forward and reverse primer sequences for qPCR.**

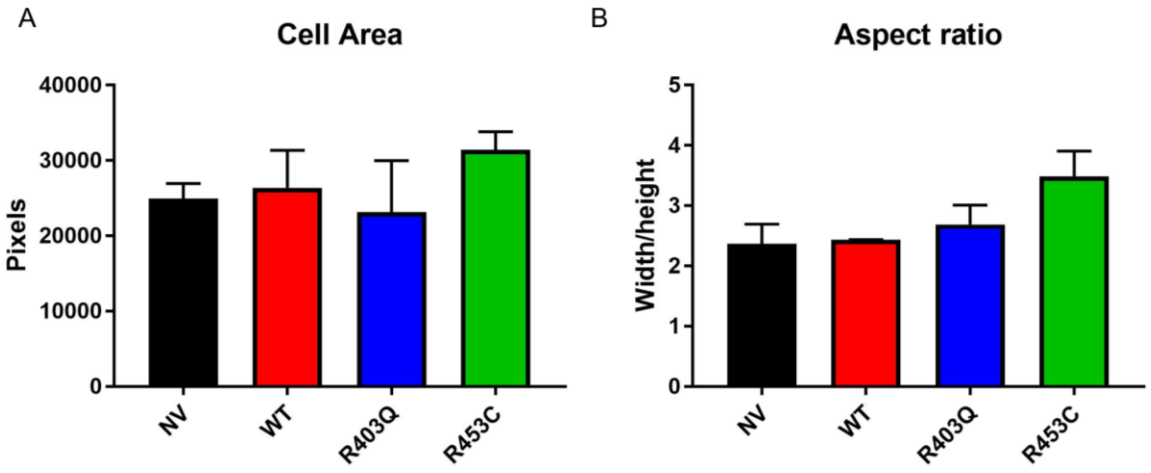

Figure S1: **Preliminary data on cell size and aspect ratio of NRVMs with HCM mutations.** a) differences in cell area b) increase trend in aspect ratio for RQ and RC compared to NV and WT

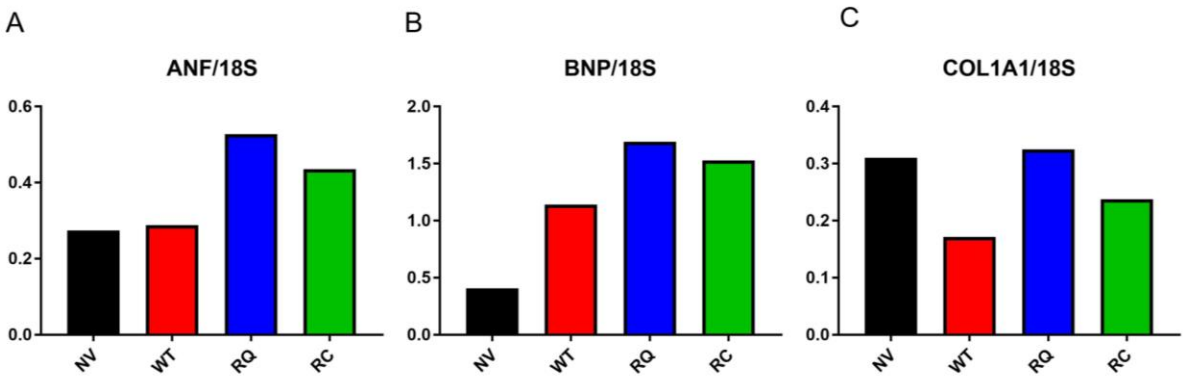

Figure S2: **Preliminary data on gene expression profiles of NRVMs with HCM mutations.** a) Relative ANF mRNA normalized to 18S RNA expression in NRVMS with no virus or WT/RQ/RC viruses b) Relative BNP expression c) Relative Collagen Type I expression